Arabian Journal of Chemistry (2020) **13**, 7007–7019

King Saud University

Arabian Journal of Chemistry

www.ksu.edu.sa
www.sciencedirect.com

ORIGINAL ARTICLE

Adsorption behavior of Pd(II) ions from aqueous solution onto pyromellitic acid modified-UiO-66-NH_2

Zhen Huang [a,c,d], Chen Wang [a,c,d], Jiling Zhao [a,c,d], Shixing Wang [a,c,d,*], Yang Zhou [b], Libo Zhang [a,c,d]

[a] *Faculty of Metallurgical and Energy Engineering, Kunming University of Science and Technology, Kunming, Yunnan 650093, China*
[b] *School of Textile Science and Engineering, National Engineering Laboratory for Advanced Yarn and Clean Production, Wuhan Textile University, Wuhan 430200, China*
[c] *State Key Laboratory of Complex Nonferrous Metal Resources Clean Utilization (Kunming University of Science and Technology), Kunming, Yunnan 650093, China*
[d] *National Local Joint Laboratory of Engineering Application of Microwave Energy and Equipment Technology, Kunming, Yunnan 650093, China*

Received 6 February 2020; accepted 4 July 2020
Available online 11 July 2020

KEYWORDS

Palladium;
Adsorption;
Mechanism;
MOF

Abstract A new adsorbent was successfully fabricated by chemically linking pyromellitic acid onto a zirconium-based metal-organic framework composite for selective adsorption of Pd(II) from an aqueous solution. The adsorbent was characterized by Fourier transform infrared spectroscopy, Brunauer–Emmett–Teller equation and scanning electron microscope. The adsorption capacity, selectivity and repeatability of the adsorbent were tested by batch experiments. The optimum pH was 2.0, and the maximum adsorption capacity at room temperature was 226.1 mg/g. In the kinetic experiments, the adsorption process achieved equilibrium within 5 h and generally conformed to the quasi-second kinetics and Freundlich isotherm model. The N-H and O—H groups on the adsorbent interacted with Pd(II) by electrostatic and coordination action. The adsorbent maintained excellent adsorption capacity after at least 5 cycles. At the same time, the selectivity of the adsorbent in aqueous solution is excellent from interfering ions. Therefore, the new adsorbent will have an obvious application prospect on the recovery of palladium.

* Corresponding author at: Faculty of Metallurgical and Energy Engineering, Kunming University of Science and Technology, Kunming 650093, China.
E-mail address: wsxkm@126.com (S. Wang).
Peer review under responsibility of King Saud University.

Production and hosting by Elsevier

https://doi.org/10.1016/j.arabjc.2020.07.007
1878-5352

1. Introduction

In today's world, palladium is an indispensable material for industry due to its specific physical and chemical properties (Morcali and Zeytuncu, 2015). These industrial activities including the electronic, catalytic and jewelry industries generate a large amount of wastewater containing Pd(II) (Das, 2010; Park et al., 2012; Won et al., 2013). On the hand, water contamination is one of the most preeminent global issues. Pd (II) solution is essentially carcinogenic and will devastate liver and kidney (Kielhorn et al., 2002; Li et al., 2018). On the other hand, the natural sources of palladium are scarce and the content of Pd(II) in wastewater is much higher than that in natural ores. Therefore, it is important to recover Pd(II) ions from aqueous solutions.

In order to recover effectively Pd(II) ions from aqueous solutions, various technologies (e.g. solvent extraction, solid phase extraction or ion-exchange, electrochemical recovery, co-precipitation, reverse osmosis, membrane separation and adsorption) have been developed (Els et al., 2000; Xie et al., 2018; Ozturk et al., 2011; Pang et al., 2018; Truong and Lee, 2018; Wu et al., 2019). In contrast, adsorption has been considered as one of the most outstanding technologies for recycling Pd(II) ions from aqueous solutions and wastewater. Because it is simplicity, less chemical sludge generation and high efficiency (Yu et al., 2019). In recent years, researchers have developed a variety of adsorbents to recover Pd(II) ions such as chitosan (Kumar et al., 2015), montmorillonite (Baki et al., 2014), silica (Dai et al., 2017) and so on. However, traditional adsorbent has limitations such as low adsorption capacity and the lack of functional and structural tunability. Therefore, it was essential to develop a new efficient absorbent.

In this regard, metal-organic frameworks (MOFs) have received more and more interests on account of its large specific area, exposed active sites and tunable pore sizes and shape (Wang et al., 2019; Zhu et al., 2017). MOFs were applied to remove a variety of pollutants such as dyes (Oveisi et al., 2017), metal ions (Bakhtiari and Azizian, 2015), organic compounds (Zhou et al., 2017), herbicides (Sarker et al., 2017) and humic acid (Abdullah et al., 2018). However, MOFs has some disadvantages, such as poor adsorption capacity, selectivity and reusability. Therefore, MOFs must be functionalized with specific functional groups. The aminated Zr-based MOF (UiO-66-NH_2) has aroused a wide research interest because of its high thermal and chemical stability, and easy functionalization (Katz et al., 2013). UiO-66-NH_2 has been covalently modified by several groups for a variety of adsorption applications. UiO-66-NH_2 functionalized by thiourea, isothiocyanate and isocyanate exhibited excellent adsorbability for heavy metal ions (Saleem et al., 2016). The dimethyl-functionalized UiO-66 showed high reliability for CO_2 uptake in comparison with analogous UiO-66 type MOFs (Huang et al., 2012). UiO-66 modified by polyurethane oligomer presents selective uptakes of hydrophilic dyes from aqueous solution (Yao et al., 2016). So, the functionalization of UiO-66-NH_2 with different active functional groups provides a promising opportunity for selective separation and capture of noble metal ions from solution.

In this research, UiO-66-NH_2 was functionalized with pyromellitic acid and used as a new adsorbents to selectively recover Pd(II) from solutions. The effect of its optimum pH, initial Pd(II) concentration and adsorption time on the uptake performance was investigated. A multi-ion solution was used to detect the selectivity of the adsorbent. In addition, the adsorption mechanism and repeatability of the adsorbent toward Pd(II) ions, as well as the isotherms and kinetics during adsorption, were investigated.

2. Experimental

2.1. Materials

Zirconium tetrachloride($ZrCl_4$), N,N-dimethylformamide (DMF) and pyromellitic anhydride were supplied by Shanghai Macklin Biochemical Co. Ltd. 2-Aminoterephthalic acid was purchased by Aladdin Chemistry Co. Ltd. Nanjing Chemical Reagent Co. Ltd. provided thiourea(99%), sodium hydroxide (99%), $PdCl_2$(60%), $CuCl_2$(99.9%), $PbCl_2$(98%) and $ZnCl_2$, hydrochloric acid(37%). All of the above reagents were of analytical grade and had not been further processed. In addition, distilled water was obtained in the laboratory.

2.2. Methods

2.2.1. Preparation of pyromellitic acid modified-UiO-66-NH_2

The functionalization of UiO-66-NH_2 was displayed in Scheme 1. Firstly, UiO-66-NH_2 was synthesized according to the reported method (Katz et al., 2013). One gram of 2-aminoterephthalic acid and one gram of zirconium tetrachloride were mixed into 50 ml of DMF. Then it was put into a three-necked reactor and hold for 24 h at 413 K. The solid was separated by centrifugation and then rinsed 5 times with DMF. After washed 5 times with absolute ethanol, the solid was dried at 350 K for 8 h. Finally, 1.5 g of pyromellitic dianhydride, 50 ml solution of DMF and 1 g of UiO-66-NH_2 were introduced to the three-necked reactor and hold for 24 h at

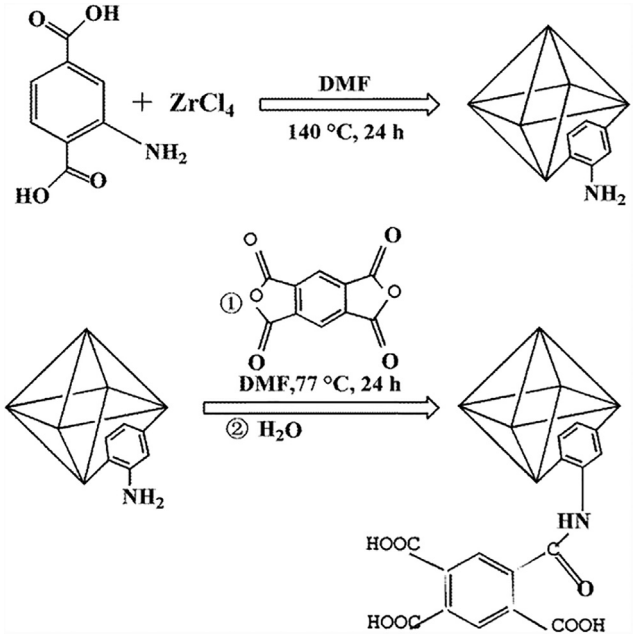

Scheme 1 Synthesis process of the pyromellitic acid modified-UiO-66-NH_2.

350 K. The solid was recovered by centrifugation and washed with DMF and distilled water 5 times. After drying for 8 h, the pyromellitic acid modified-UiO-66-NH_2 was obtained.

2.2.2. Adsorption test

Batch experiments were implemented at room temperature. The pyromellitic acid modified-UiO-66-NH_2(10 mg) was mixed with 15 ml of Pd(II) ions solution(100 mg/L) and shaken at 280 rpm. After separated at 9800 rpm for 3 min, the residual Pd(II) ions in the solution were measured by atomic absorption spectrum (AAS). Eqs. (1) and (2) are used to calculate removal the rate (R%) and the adsorption capacity at equilibrium (q_b mg/g):

$$R = \frac{c_0 - c_r}{c_0} \times 100\% \quad (1)$$

$$q_b = \frac{c_0 - c_r}{m} \times v \quad (2)$$

The initial and remaining concentrations of Pd(II) ions were replaced by C_0 (mg/L) and C_r (mg/L), respectively. V (L) is the solution volume and m (mg) is the weight of the pyromellitic acid modified-UiO-66-NH_2.

2.3. Characterization methods

Nicolet iS50 Fourier transform infrared spectrometer (FT-IR, USA) was applied to record the change of the infrared spectrum for UiO-66-NH_2 during the modification. Brunauer–E mmett–Teller equation (BET) measured the BET surface area of the samples. The non-local density functional theory (NLDFT) analyzed the pore size. The morphology of the metal organic framework composite was analyzed by JSM-7100F (JEOL). Zeta potential analyzer (Brookhaven Instruments Co., Austin, TX, America) were employed to detect the isoelectric points of the pyromellitic acid modified-UiO-66-NH_2. The ions concentrations was detected by atomic absorption spectrum (AAS,AA-7000) and XPS (Thermo Scientific Co., 1486.6 eV radiation source of monochromatized Al K-alpha, U.S.A) was used to investigate the surface chemical states of the pyromellitic acid modified-UiO-66-NH_2.

3. Results and discussion

3.1. *Characteristic of* the pyromellitic acid modified-UiO-66-NH_2

FT-IR spectra of UiO-66-$NH_2$and the pyromellitic acid modified-UiO-66-NH_2 were collected Fig. 1. The absorption bands at 3456 cm^{-1} and 3348 cm^{-1} derived from the symmetrical and asymmetrical stretching vibration of —NH_2 in FT-IR spectra of UiO-66-NH_2 (Jermakowicz-Bartkowiak, 2005; Tang et al., 2000). The peak at 1656 cm^{-1} came from the N-H bond. The absorption band at 1572 cm^{-1} derived from asymmetric vibration of the carboxyl groups. The absorption band at 1385 cm^{-1} originated from C—O bond (carboxylic acid). The absorption band at 1258 cm^{-1} originated from the stretching vibration of C—N (Xavier and Gobinath, 2012). After modification with pyromellitic acid, the absorption bands at 3456 cm^{-1} and 3348 cm^{-1} (—NH_2) disappeared, and a new absorption band appeared at 3372 cm^{-1} (—OH/O—H). Obviously, the disappearance of the absorption band at 1656 cm^{-1} and the enhanced intensity of absorption band at 1572 cm^{-1} certified the reactions of amino and carboxyl groups.

The pore size distribution is crucial for the adsorption capacity (Jeong et al., 2012). Therefore, the BET is test (Fig. 1a and Table 1). The pyromellitic acid modified-UiO-

Table 1 Surface area, average pore radius and total pore volume of UiO-66-NH_2 and the pyromellitic acid modified-UiO-66-NH_2.

Category	UiO-66-NH_2	The pyromellitic acid modified-UiO-66-NH_2
Surface area (m^2/g)	702.21	396.71
Average pore Radius (nm)	1.17	1.08
Total pore volume (cm^3/g)	4.11	2.14

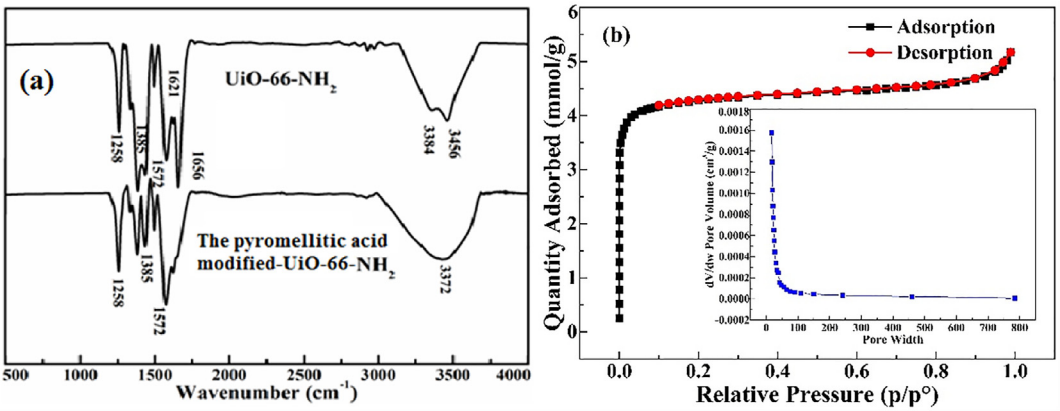

Fig. 1 FT-IR spectra of UiO-66-NH_2 and the pyromellitic acid modified-UiO-66-NH_2 (a) and BET of the pyromellitic acid modified-UiO-66-NH_2 (b).

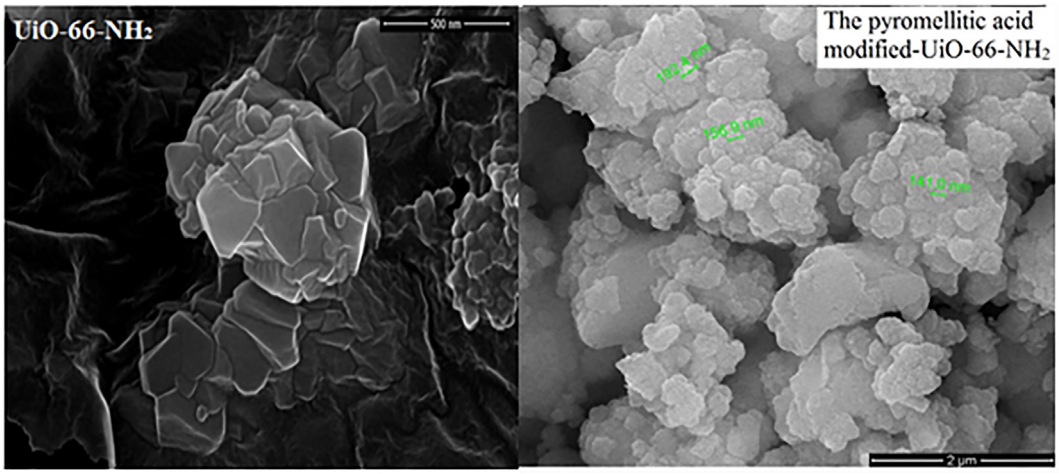

Fig. 2 The scanning electron micrograph of UiO-66-$NH_2$and the pyromellitic acid modified-UiO-66-NH_2.

66-NH_2 had an excellent average pore diameter of 1.08 nm and is microporous. At the same time, the specific surface area of the pyromellitic acid modified-UiO-66-NH_2 is 282.08 m^2/g. Fig. 2 is the scanning electron image of UiO-66-NH_2 and the pyromellitic acid modified-UiO-66-NH_2. Their sizes were 2.4 6 ± 0.64 nm and there was no obvious difference in the size. This showed that the adsorbent maintains good stability after post-modification.

3.2. Influence of initial pH on adsorption

The actual pH value of the solution has a remarkable influence on adsorption property by interacting with the active functional groups of the adsorbent. Especially, pH will affect the species and surface charge of palladium ions. In order to avoid the hydrolysis of Pd(II), the pH value is set between 1.0 and

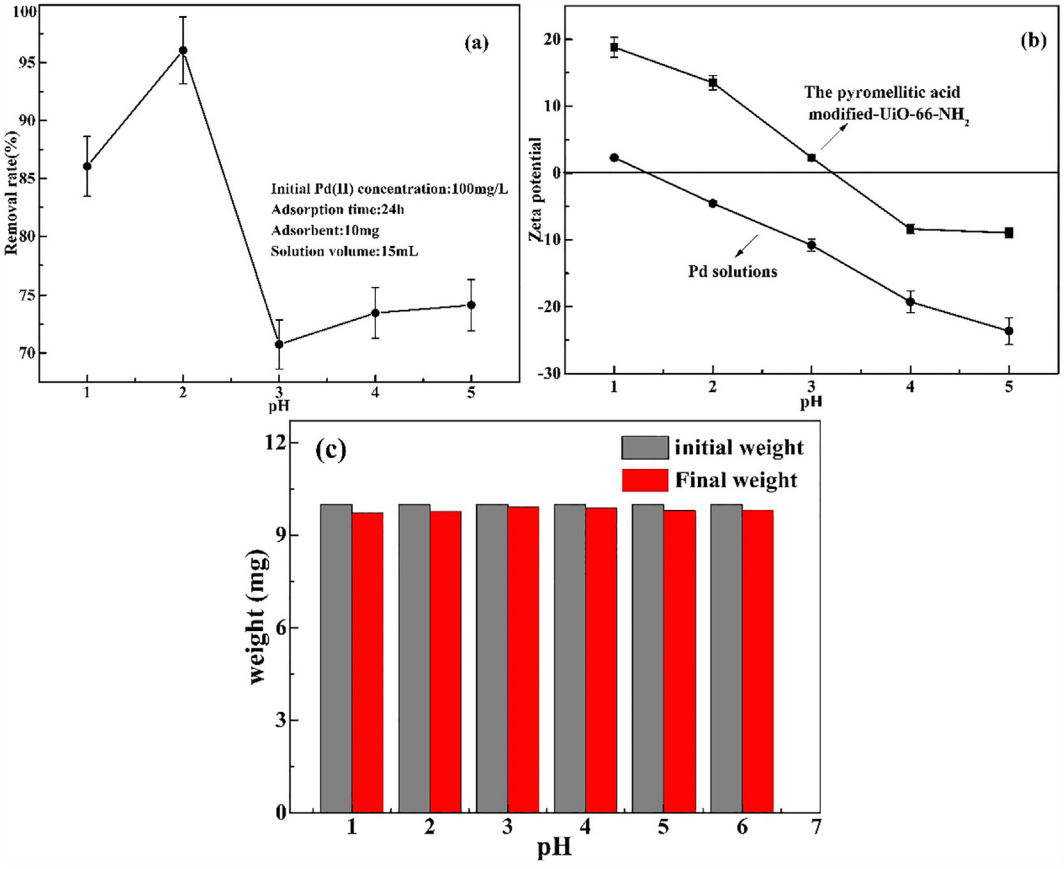

Fig. 3 Influence of solution pH (a) and zeta potential (b) and Acid-base stability (c) of the pyromellitic acid modified-UiO-66-NH_2. (pH:1–5, Temperature: 298 K, Time: 24 h, Pd(II) concentration: 100 mg/L).

5.0. 10 mg of the pyromellitic acid modified-UiO-66-NH_2 was added to Pd(II) solution(15 ml) and shaken for 24 h at room temperature. After separated, the remaining Pd(II) concentration was measured. Fig. 3a displayed the influence of different pH values on adsorption. The removal rate of Pd(II) increased when the pH values changed from 1.0 to 2.0. The hydrogen ions competed the anchoring sites with Pd(II) at lower pH, resulting in the decrease of the adsorption capacity(Sharma and Rajesh, 2016). The adsorption percentage of Pd(II) was significantly reduced at a pH greater than 2.0, which can be attributed to the competition of hydroxyl complexes such as $PdCl_2(OH)^{2-}$, $Pd(OH)_2$ and $Pd(OH)_4^{2-}$ for active adsorption sites(Hubicki and Wołowicz, 2009). The removal rate had only a slight increase in the pH range of 3.0 to 5.0. So, the optimal pH was 2.0.

For exploring the adsorption mechanism of Pd(II), Zeta potential of the pyromellitic acid modified-UiO-66-NH_2 was detected in different pH solutions. The equipotential of the pyromellitic acid modified-UiO-66-NH_2 was at pH 3.2 (Fig. 3b). When the pH was less than 3.2, the pyromellitic acid modified-UiO-66-NH_2 was positive in aqueous solution. Correspondingly, the Pd(II) solution began to be negative after the pH was greater than 1.3. When the pH was greater than 3.2, the pyromellitic acid modified-UiO-66-NH_2 was negative in water, while the Pd(II) solution was still negative. So, there was electrostatic interaction between Pd(II) ions and the pyromellitic acid modified-UiO-66-NH_2 in the range of pH from 1.3 to 3.2. When the pH was too low, high concentrations of hydrogen ions compete with Pd(II) ions for adsorption sites on the pyromellitic acid modified-UiO-66-NH_2. When the pH was too high, the carboxyl group on the surface of the pyromellitic acid modified-UiO-66-NH_2 was electronegative, leading to electrostatic repulsion between palladium ions and the pyromellitic acid modified-UiO-66-NH_2.

Fig. 3c is the stability experiment of adsorbent based on the change of mass. 10 mg the pyromellitic acid modified-UiO-66-NH_2 was mixed with 15 ml water in the range of pH from 1 to 6 and shake for 24 h. After centrifugation and drying, the mass of the solid was weighed. As can be seen from the figure, the weight of the adsorbent has decreased within the experimental error. It may be caused by the operation during the experiment. It shows that the pyromellitic acid modified-UiO-66-NH_2 has good stability at different pH.

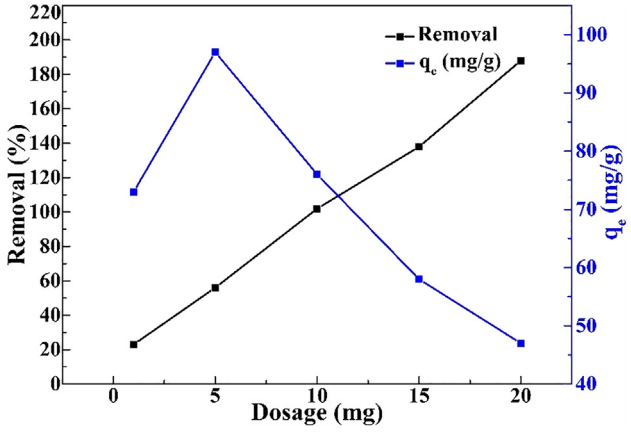

Fig. 4 The effect of the amount of adsorbent on adsorption (pH: 2, Temperature: 298 K, Time: 24 h, Pd(II) concentration: 100 mg/L).

3.3. Influence of the amount of adsorbent

In order to study the influence of the amount of adsorbent, the Pd(II) concentration is100 mg/L and pH is 2.0. The dosage of adsorbent ranges from 1 to 20 mg and the adsorption time is 24 h at 298 K. Fig. 4 indicated the effect of adsorbent dosage on Pd(II) uptake and removal percentage. The adsorption capacity decreases with an increase in the adsorbent dosage from 1 to 20 mg. The maximum uptake was achieved with 5 mg and the minimum uptake occurred at 20 mg dosage. Therefore, the number of Pd(II) adsorbed on the adsorbent decreased when the dosage of adsorbent increased, leading to lower uptake. On the other hand, the removal efficiency enhanced from 21.4% to 97.2% with the increase of the dosage. The maximum Pd(II) removal occurred at the greatest dose (20 mg). This is due to an increase in the available active adsorption sites.

3.4. Influence of adsorption time and adsorption kinetics

The influence of the adsorption time was explored. 10 mg of the pyromellitic acid modified-UiO-66-NH_2 was put into 15 ml of Pd(II) solution (100 mg/L) at 298 K. Experiments were mainly conducted between 0 and 900 min. The removal efficiency of Pd(II) reached half of the maximum adsorption capacity at 30 min, and then the adsorption speed was slowed down (Fig. 5a). Finally the adsorption equilibrium was attained at 300 min. Before the adsorption equilibrium (300 min) was achieved, the adsorption sites on the pyromellitic acid modified-UiO-66-NH_2 surface are sufficient, but the contact time was limited, resulting in only the part adsorption of the Pd(II) ions. As the adsorption time continued to lengthen, the contact sites were in full contact with the Pd (II) ions until the adsorption equilibrium is reached. After 300 min, the adsorption sites on the surface of the the pyromellitic acid modified-UiO-66-NH_2 were fully occupied and no more Pd(II) ions were adsorbed.

For exploring the adsorption mechanism of Pd(II), the adsorption kinetics was investigated by the three models. Lagrange's pseudo-first order model was represented by Eq. (3) for adsorption of various liquid-solid systems (Wang et al., 2010). The pseudo second-order model contains the equilibrium equation of mass and the second derivative of rate and the control step is chemisorption (Shahwan, 2014). Eq. (4) is used to represent the pseudo second-order model. The rate of adsorption was dominated by intraparticle diffusion in some system with high concentration of adsorbate, intense agitation and larger adsorbents (Malash and El-Khaiary, 2010). Eq. (5) is used to represent the intraparticle diffusion model.

$$In(q_b - q_t) = Inq_b - k_1 t \tag{3}$$

$$\frac{t}{q_t} = \frac{1}{k_2 q_b^2} + \frac{t}{q_b} \tag{4}$$

$$q_t = k_i t^{1/2} + D \tag{5}$$

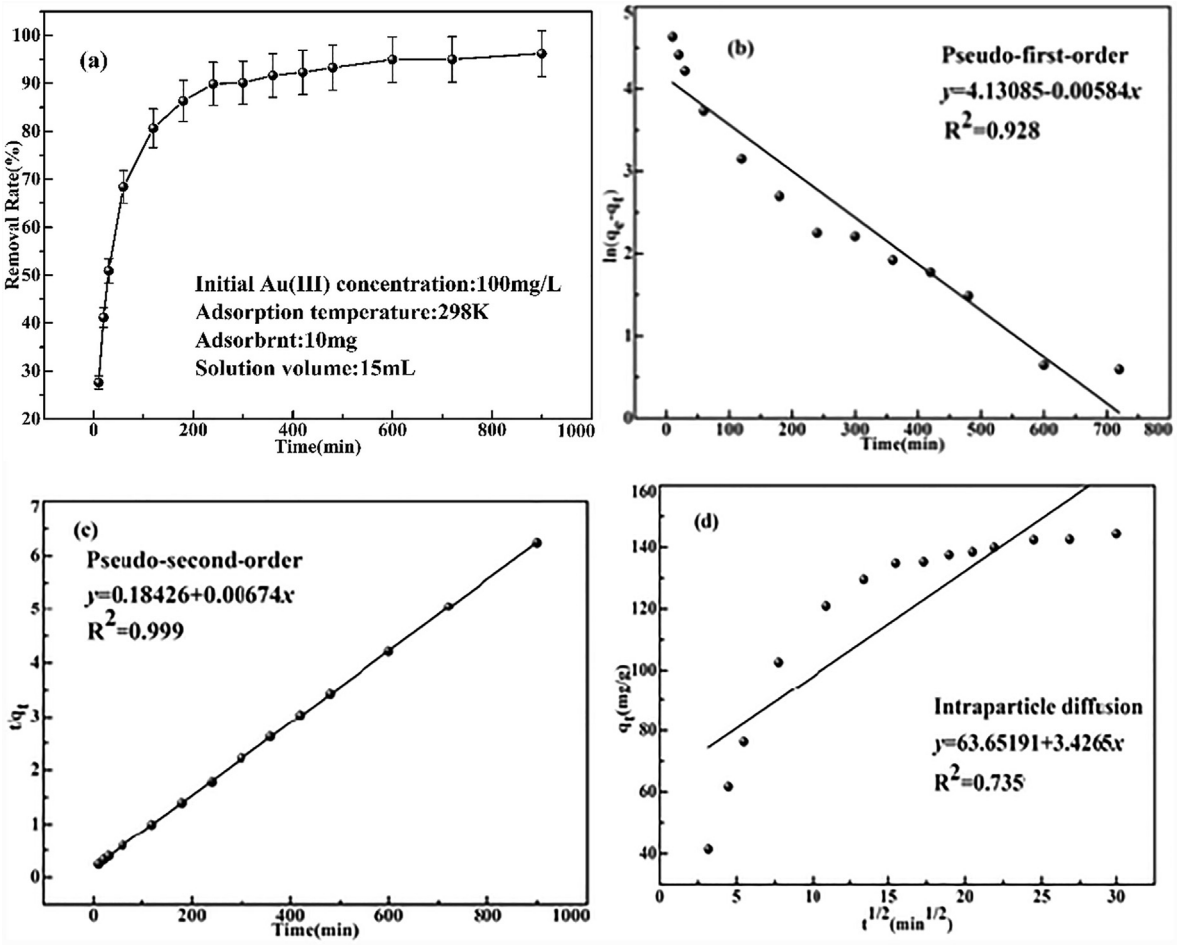

Fig. 5 (a) Influence of absorption time on adsorption capacity; (b) Pseudo-first-order model; (c) Pseudo-second-order model; (d) Intraparticle diffusion model (pH:2, Temperature: 298 K, Pd(II) concentration: 100 mg/L).

The adsorption capacity of Pd(II) at time t and equilibrium time are represented by q_t and $q_{b,}$ respectively. k_1, k_2 and $k_i$denoted the rate constants of the pseudo first/second-order and intraparticle diffusion models, respectively. The boundary layer thickness is expressed by D.

The corresponding parameters of the kinetics equations are shown in Table 2, and the linear relationship is shown in Fig. 5b–d. Their correlation coefficient (R^2) presented such a relationship: intraparticle diffusion (0.73594) < pseudo first-order (0.92834) < pseudo second-order (0.9995). The equilibrium adsorption capacity of the pseudo second-order model (148.37 mg/g) is far higher than that of the pseudo first-order model (62.23 mg/g). Moreover, the actual equilibrium adsorption capacity was 144.32 mg/g, which was close to the data of the pseudo second-order model. Therefore, the Pd(II) adsorption can well be explained by the pseudo second-order model. The chemisorption is the determining step. That is to say, the interaction between Pd(II) ions and the recognition groups mainly rely on the chemical interaction. As can be seen from Fig. 4d, the linear relationship of the intraparticle diffusion model can be divided into three regions. In the region I ($t \leq 60$ min), there are sufficient anchoring sites on the surface of the pyromellitic acid modified-UiO-66-NH_2, so the adsorption capacity increases sharply with time. Region II (60 min $\leq t \leq$ 240 min) showed a gradual decrease in adsorption capacity due to a decrease in available binding sites. In the region III (240 min $\leq t \leq$ 9000 min), the adsorption equilibrium is gradually reached. The intercepts of the three regions all exceed 0, so that the whole adsorption process is complicated, and it is known that intraparticle diffusion is also a factor for controlling the adsorption rate (Harja and Ciobanu, 2018).

Table 2 The parameters of kinetics models.

Kinetics model	Parameters	Values
Pseudo-first-order	k_1	−0.0058
	R^2	0.928
	q_e	62.23
Pseudo-second-order	k_2	0.0067
	R^2	0.999
	q_e	148.37
Intraparticle diffusion	k_3	3.43
	R^2	0.736

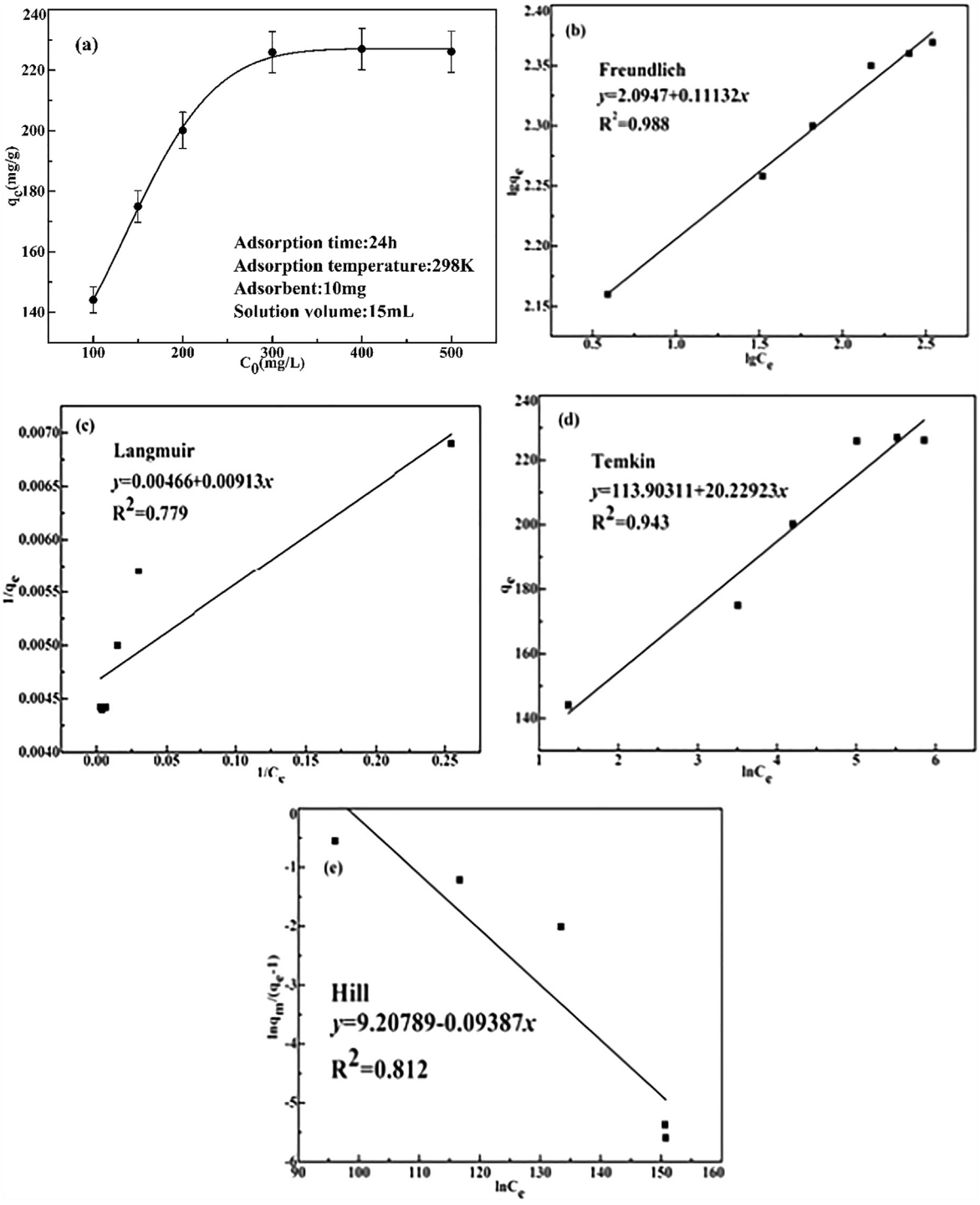

Fig. 6 Influence of initial Pd(II) concentration (a), linearized Freundlich (b), Langmuir (c), Temin (d) and Hill (e) isotherm models for Pd(II) adsorption on the pyromellitic acid modified-UiO-66-NH_2. (pH: 2, Temperature: 298 K, Time: 24 h).

3.5. Influence of initial concentration and adsorption isotherms

The initial Pd(II) concentration also had an effect on the adsorption capacity. 10 mg of the pyromellitic acid modified-UiO-66-NH_2 was put into Pd(II) ions solutions with different concentrations (100, 150, 200, 300, 400, and 500 mg/L). It was seen from Fig. 6a, as the concentration of Pd(II) ions increased, the adsorption capacity of the adsorbent increased. When the Pd(II) ion concentration was low, the Pd(II) ions were insufficient to the anchoring sites on the adsorbent. However, as the concentration increased, the anchoring sites on the adsorbent and the Pd(II) ions were fully combined and saturated at 300 mg/L. The maximum adsorption capacity of Pd (II) is 226.1 mg/g.

This adsorption isotherm indicated that the interacted way of the adsorbent with the Pd(II) ion and expressed the relation-

ship between the adsorption capacity and concentration. The Freundlich, Langmuir, Temkin and Hill isotherm models are used to study the adsorption capacity and equilibrium Pd(II) concentration at pH 2.0. The Freundlich equation describes heterogeneous systems and reversible adsorption, both multilayer and monolayer (Wang et al., 2016). The Langmuir adsorption isotherm described that adsorption is a single layer adsorption on an identical surface, adsorption-desorption maintain a dynamic equilibrium (Arief et al., 2010). Temkin equation presumed that the molecules adsorption heat would linearly decline with the fraction of coverage in the layer because the interaction between very low and very large concentration values was neglected (Araújo et al., 2018). The Hill isotherm model describes the relationship of different adsorbents on a uniform surface and the correlation between the ligand binding capacity of a site and the different adsorption sites on the surface (Tanzifi et al., 2017). The following linear Eqs. (6), (7), (8) and (9) respectively represented the isotherms of the Freundlich, Langmuir, Temkin and Hill isotherm models:

$$\lg q_b = \lg K_F + \frac{1}{n}\lg C_b \tag{6}$$

$$\frac{1}{q_b} = \frac{1}{q_m} + \frac{1}{K_L q_m}\cdot\frac{1}{C_b} \tag{7}$$

$$q_b = B_T In K_T + B_T In C_b \tag{8}$$

$$In\left(\frac{q_m - q_b}{qb}\right) = In K_G + N In C_f \tag{9}$$

In these equations, C_b is the equilibrium concentration of Pd(II). K_F is a constant related to q_e, n is the adsorption intensity, the maximum adsorption quantity is expressed by q_m, K_L is the Langmuir invariant, $B_T$andK_T is the adsorption heat and the equilibrium association constant, respectively. K_G is the constant of Hill model.

Fig. 6b–e showed the Linear curve of four isotherm models and their related parameters were listed in Table 3. Their correlation coefficient (R^2) presented such a relationship: Langmuir < Hill < Temkin < Freundlich. According to the correlation coefficientsR^2 (closest to 1) and 1/n (between 0.1 and 0.5) of Freundlich, the adsorption the pyromellitic acid modified-UiO-66-NH_2 for Pd(II) ions preferentially obeyed Freundlich model (Srivastava et al., 2017). The process conformed to a multilayer adsorption or heterogeneous system or reversible adsorption. Finally, the Pd(II) ions adsorbents in other literatures was listed in Table 4 for comparison. It can be found that although the adsorption equilibrium time of the pyromellitic acid modified-UiO-66-NH_2 is long, it has excellent adsorption ability.

Table 3 The parameters of different isotherms models.

Isotherm Model Parameter	Parameter	Value
Freundlich	$K_F(mg{\cdot}g^{-1}(L\cdot mg^{-1})^{1/n})$	8.12
	1/n	0.11
	R^2	0.988
Langmuir	K_L(L/g)	1.96
	R^2	0.780
Temkin	B_T(J/mol)	20.23
	K_T(L/g)	1.00
	R^2	0.944
Hill	K_G(L/g)	9975.53
	N	−0.094
	R^2	0.813

Table 4 Comparison of the adsorption capacity for the Pd(II) ions onto the pyromellitic acid modified-UiO-66-NH_2 and other adsorbents reported in literature.

adsorbents	q_{max} (mg/g)	Adsorption time (min)	References
EPPFR	112.6	60	(Yi et al., 2016)
PPF resin	111.11	840	(Xie et al., 2016)
PEI-PSBF	216.9	240	(Cho et al., 2016)
Glcine modified crosslinked chitosan resin	120.39	120	(Ramesh et al., 2008)
PEI-modified biomass	176.8	30	(Won et al., 2011)
the pyromellitic acid modified-UiO-66-NH_2	226.1	300	This work

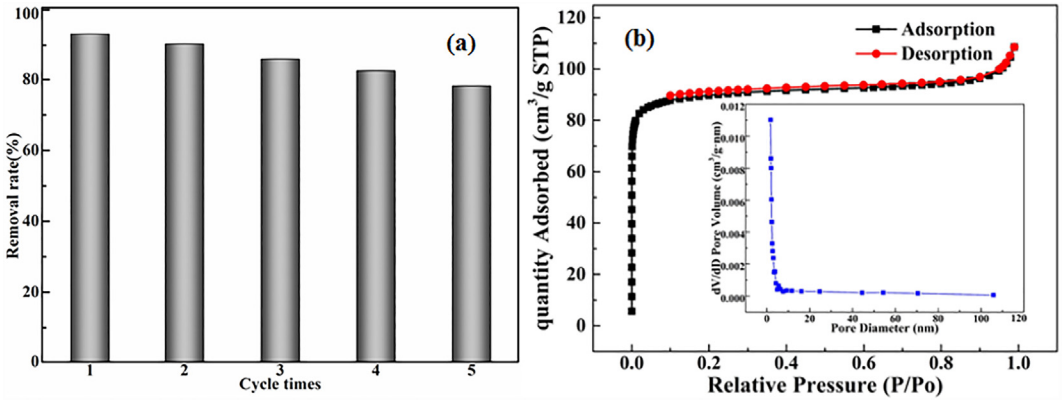

Fig. 7 Reusability (a) and BET after adsorption (b) of the pyromellitic acid modified-UiO-66-NH_2.

3.6. Desorption and recyclability

In practical applications, the regenerative capacity is indispensable for adsorbents. Thiourea is an important eluent for Pd(II) ions because it has strong chelating action with Pd(II) ions. 50 mg of the pyromellitic acid modified-UiO-66-NH_2 was put to 75 ml of a Pd(II) solution (100 mg/L) and shake for 10 h. Pd(II) ion concentration in supernatant was measured. Then, the precipitate was eluted with a thiourea eluent for 10 h and washed with distilled water 5 times to obtain a regenerated adsorbent. After five repetitions, the Pd(II) removal rate was reduced from 93.2% to 78.2% (Fig. 7a). This shows that the pyromellitic acid modified-UiO-66-NH_2 had good stability and regenerability, and could maintain good adsorption capacity after repeated regeneration. The weight of adsorbent was decreased by 5.2 mg after 5 cycles. The specific surface area, pore diameter and pore volume of the adsorbent decrease to 273.59 m^2/g, 2.46 nm and 0.12 cm^3/g (Fig. 7b). These led to the reduction of the reusability of the adsorbent.

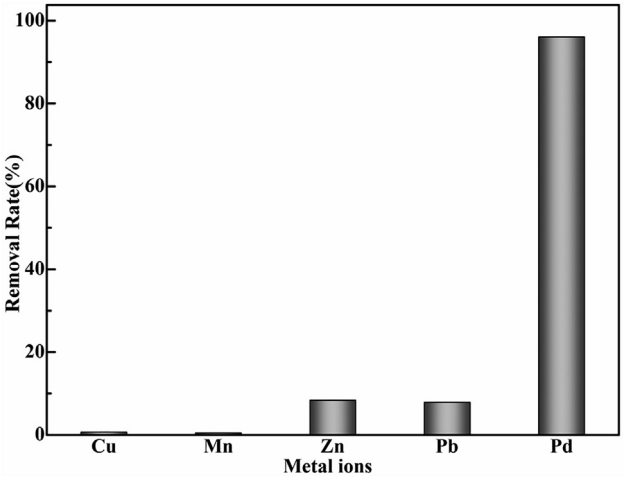

Fig. 8 . Selective recovery of Pd(II) from aqueous solutions.

3.7. Selective adsorption

The adsorption selectivity of Pd(II) ions was explored from a solution including Cu(II), Mn(II), Zn(II), Pb(II) and Pd(II). The concentration of all ions is 100 mg/L. Ten mg of the pyromellitic acid modified-UiO-66-NH_2 was put to 15 ml binary system containing various ions. It was shaken at pH 2.0 for 24 h. After centrifugation, the concentration of all metal ions in supernatant was measured. The adsorption capacity of Pd (II) exceeded that of other ions (Fig. 8).

$$K_d = \frac{q}{C_f} = \frac{C_i - C_f}{C_f} \cdot \frac{V}{m} \tag{10}$$

$$K = \frac{K_{d(Au)}}{K_{d(coexisting\ -\ ion)}} \tag{11}$$

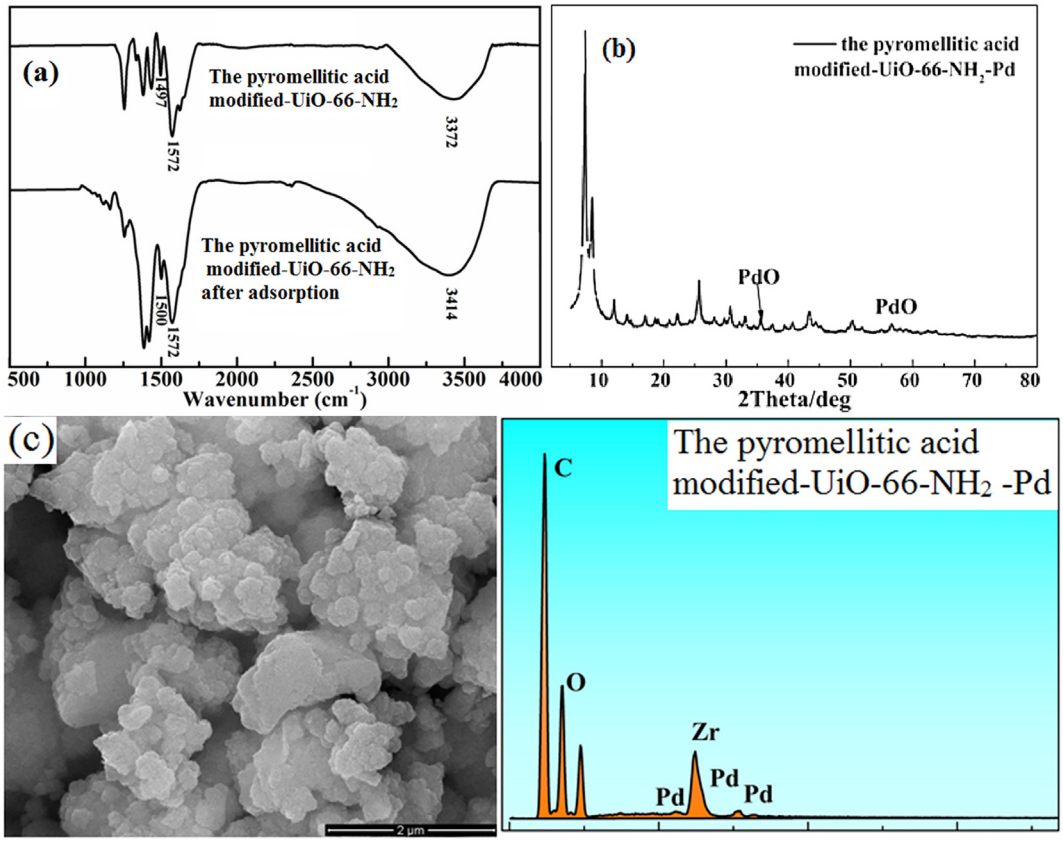

Fig. 9 Infrared spectra (a) and XRD after adsorption (b) and SEM-EDS (c) of the pyromellitic acid modified-UiO-66-NH_2 after adsorption.

Table 5 The values of K_d and K of metal ions.

Coexisting ions	K_d (mL/g)	K
Pd^{2+}	36670.9	–
Cu^{2+}	9.7909	3745.4
Mn^{2+}	6.7366	5443.5
Zn^{2+}	143.437	255.66
Pb^{2+}	133.84	273.99

The selection coefficient (K) and the distribution coefficient (K_d) are obtained by Eqs. (10) and (11) (Zhang et al., 2017). q and C_f respectively represent the adsorption capacity and residual concentration of the ions. K_d and K of each metal ion were collected in Table 5. The pyromellitic acid modified-UiO-66-NH_2 owns good selectivity for Pd(II) ions from a interfering ion solution. The zeta potential of Cu^{2+}, Mn^{2+}, Zn^{2+}, Pb^{2+} and the pyromellitic acid modified-UiO-

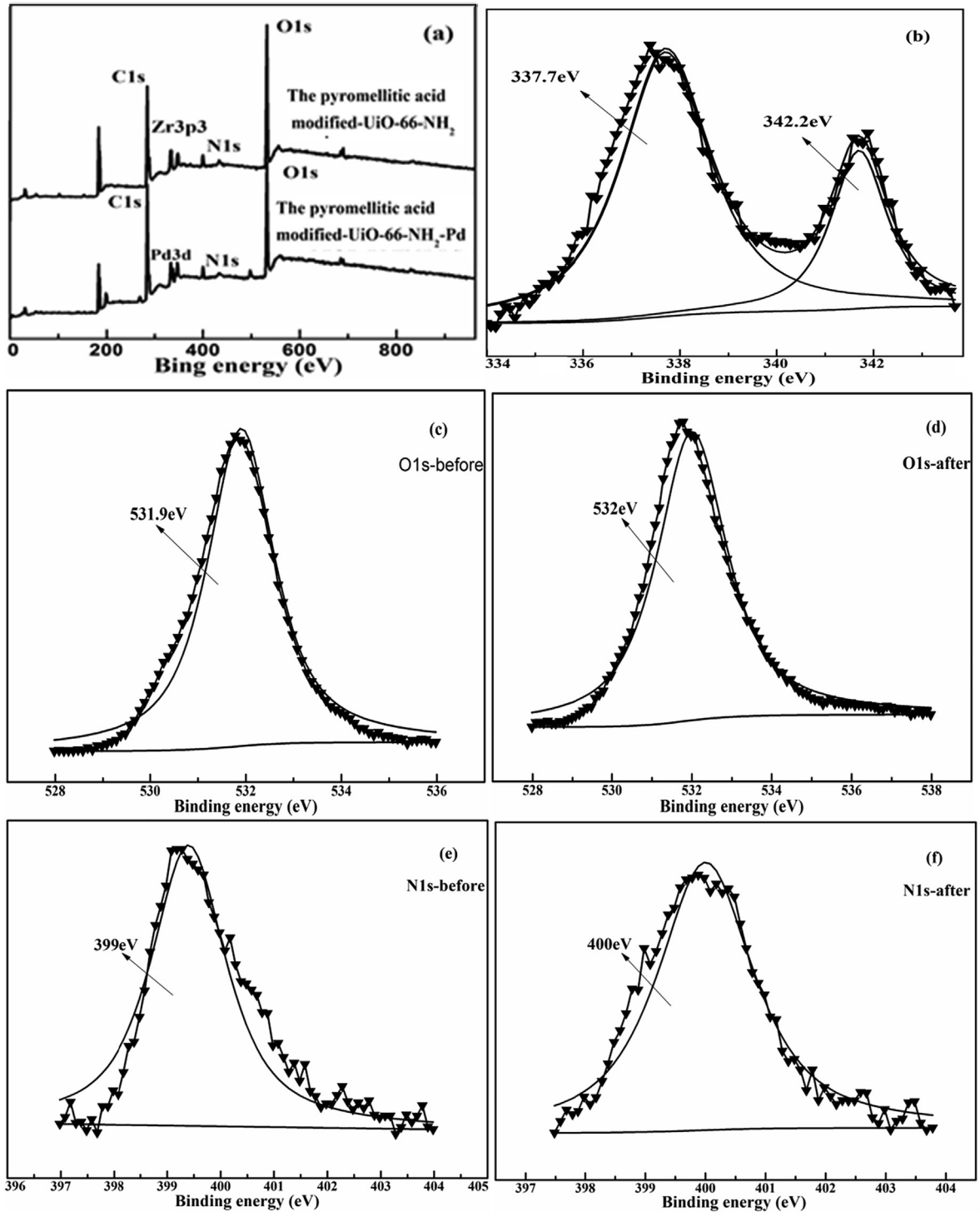

Fig. 10 XPS analysis of full spectrum, Pd3d, O1s and N1s of the pyromellitic acid modified-UiO-66-NH_2 before and after adsorption.

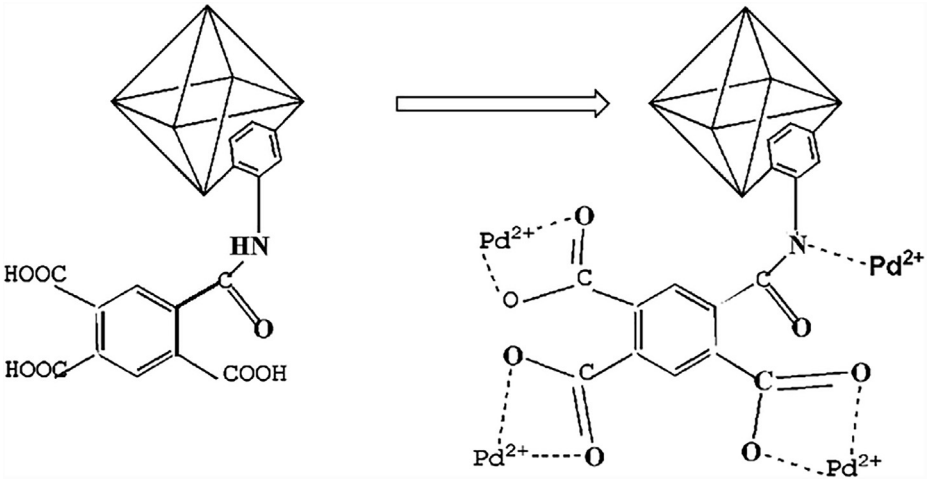

Scheme 2 Adsorption mechanism of Pd(II) ions onto the pyromellitic acid modified-UiO-66-NH_2.

66-NH_2 is positive at pH 2. The mutual repulsion decreases the adsorption of the pyromellitic acid modified-UiO-66-NH_2 for the interfering ions.

3.8. Adsorption mechanism

The infrared spectra of the pyromellitic acid modified-UiO-66-NH_2 are shown in Fig. 9a before and after adsorption. After adsorption of Pd(II) ions, the peaks of O—H and N—H groups at 3372 cm^{-1} and 1497 cm^{-1} moved to 3414 cm^{-1} and 1500 cm^{-1}, respectively. The shift was ascribed to the coordination between palladium ions and N(O)—H groups. Fig. 9b is the XRD pattern after adsorption of Pd(II). The peaks at 35.6° and 57.1° in the figure are the peaks belonging to Pd—O (Mao et al., 2020). Fig. 9c is the SEM-EDS image after adsorption. It can be seen from the figure that Pd(II) is adsorbed on the adsorbent.

XPS was also used for analysis the Pd(II) adsorption mechanism. After absorption of Pd(II), a peaks of Pd(II) at 337.7 eV appeared(Fig. 10a). Pd(II) is successfully adsorbed by the pyromellitic acid modified-UiO-66-NH_2. As shown in Fig. 10b, XPS of Pd3d is mainly composed of two peaks (337.7 eV and 342.2 eV) (Dobrzyńska et al., 2019). They correspond to Pd-N and Pd-O (oxide or hydroxide) compounds, respectively. In Fig. 10c, d, the peak of C—O—H shifted from 531.9 eV to 520 eV(Xu et al., 2017). In Fig. 10e, f, the N—H peak also slightly shifted from 399 eV to 400 eV. XPS indicated also that there is coordination between Pd(II) ions and N—H, O—H groups. So, the adsorption mechanism of Pd(II) ions on the pyromellitic acid modified-UiO-66-NH_2 is mainly the coordination and electrostatic interaction between Pd(II) ions and N-H,O-H groups(Scheme 2).

4. Conclusions

A new MOF adsorbent was synthesized by modifying UiO-66-NH_2 with pyromellitic anhydride to selectively adsorb Pd (II) from water. The maximum adsorption capacity of Pd (II) was 226.1 mg/g at pH = 2. Adsorption equilibrium was reached within 5 h. The calculation of the adsorption model shows that the adsorption isotherm is good agreement with the Freundlich model, and the adsorption kinetics is good agreement with the pseudo-second-order kinetic model. The process is mainly control by multilayer chemisorption. Moreover, the pyromellitic acid modified-UiO-66-NH_2 has good reusability and selectivity. The coordination and electrostatic interactions between ions and N-H, O-H groups are adsorption mechanisms. In short, the pyromellitic acid modified-UiO-66-NH_2 has broad prospects for the recovery of Pd (II) from water.

Declaration of Competing Interest

The authors declare that they have no known competing financial interests or personal relationships that could have appeared to influence the work reported in this paper.

Acknowledgements

This work was supported by the National Natural Science Foundation of China (51664037).

References

Abdullah, N., Rahman, M.A., Othman, M.H.D., Jaafar, J., Aziz, A. A., 2018. Preparation, characterizations and performance evaluations of alumina hollow fiber membrane incorporated with UiO-66 particles for humic acid removal. J. Membr. Sci. 563, 162–174.

Araújo, C.S.T., Almeida, I.L.S., Rezende, H.C., Marcionilio, S.M.L. O., Léon, J.J.L., Matos, T.N.D., 2018. Elucidation of mechanism involved in adsorption of Pb(II) onto lobeira fruit (Solanum lycocarpum) using Langmuir, Freundlich and Temkin isotherms. Microchem. J. 137, 348–354.

Arief, V.O., Trilestari, K., Sunarso, J., Indraswati, N., Ismadji, S., 2010. Recent progress on biosorption of heavy metals from liquids using low cost biosorbents: characterization, biosorption parameters and mechanism studies. Clean – Soil Air Water 36, 937–962.

Bakhtiari, N., Azizian, S., 2015. Adsorption of copper ion from aqueous solution by nanoporous MOF-5: a kinetic and equilibrium study. J. Mol. Liq. 206, 114–118.

Baki, M.H., Shemirani, F., Khani, R., Bayat, M., 2014. Applicability of diclofenac–montmorillonite as a selective sorbent for adsorption of palladium(II); kinetic and thermodynamic studies. Anal. Methods 6, 1875–1883.

Cho, C.W., Kang, S.B., Kim, S., Yun, Y.S., Won, S.W., 2016. Reusable polyethylenimine-coated polysulfone/bacterial biomass composite fiber biosorbent for recovery of Pd(II) from acidic solutions. Chem. Eng. J. 302, 545–551.

Dai, Y., Liu, Y., Zhang, A., 2017. Preparation and characterization of a mesoporous silica-polymer crown impregnated material and its adsorption for palladium from highly acid medium. J. Porous Mater. 24, 1037–1045.

Das, N., 2010. Recovery of precious metals through biosorption — a review. Hydrometallurgy 103, 180–189.

Dobrzyńska, J., Dobrowolski, R., Olchowski, R., Zięba, E., Barczak, M., 2019. Palladium adsorption and preconcentration onto thiol- and amine-functionalized mesoporous silicas with respect to analytical applications. Microporous Mesoporous Mater. 274, 127–137.

Els, E.R., Lorenzen, L., Aldrich, C., 2000. Adsorption of precious metals and base metals on a quaternary ammonium group ion exchange resin. Miner. Eng. 13, 401–414.

Harja, M., Ciobanu, G., 2018. Studies on adsorption of oxytetracycline from aqueous solutions onto hydroxyapatite. Sci. Total Environ. 628–629, 36–43.

Huang, Y., Qin, W., Li, Z., Li, Y., 2012. Enhanced stability and CO affinity of a UiO-66 type metal–organic framework decorated with dimethyl groups. Dalton Trans. 41, 9283–9285.

Hubicki, Z., Wołowicz, A., 2009. A comparative study of chelating and cationic ion exchange resins for the removal of palladium(II) complexes from acidic chloride media. J. Hazard. Mater. 164, 1414–1419.

Jeong, S., Kim, H., Bae, J.H., Kim, D.H., Peden, C.H.F., Park, Y.K., Jeon, J.K., 2012. Synthesis of butenes through 2-butanol dehydration over mesoporous materials produced from ferrierite. Catal. Today 185, 191–197.

Jermakowicz-Bartkowiak, D., 2005. Preparation, characterisation and sorptive properties towards noble metals of the resins from poly (vinylbenzyl chloride) copolymers. React. Funct. Polym. 62, 115–128.

Katz, M.J., Brown, Z.J., Colón, Y.J., Siu, P.W., Scheidt, K.A., Snurr, R.Q., Hupp, J.T., Farha, O.K., 2013. A facile synthesis of UiO-66, UiO-67 and their derivatives. Chem. Commun. 49, 9449–9451.

Kielhorn, J., Melber, C., Keller, D., Mangelsdorf, I., 2002. Palladium–a review of exposure and effects to human health. Int. J. Hyg. Environ. Health 205, 417–432.

Kumar, A.S., Sharma, S., Reddy, R.S., Barathi, M., Rajesh, N., 2015. Comprehending the interaction between chitosan and ionic liquid for the adsorption of palladium. Int. J. Biol. Macromol. 72, 633–639.

Li, J., Wang, X., Zhao, G., Chen, C., Chai, Z., Alsaedi, A., Hayat, T., Wang, X., 2018. Metal–organic framework-based materials:superior adsorbents for the capture of toxic and radioactive metal ions. Chem. Soc. Rev. 47, 2322–2356.

Malash, G.F., El-Khaiary, M.I., 2010. Piecewise linear regression: a statistical method for the analysis of experimental adsorption data by the intraparticle-diffusion models. Chem. Eng. J. 163, 256–263.

Morcali, M.H., Zeytuncu, B., 2015. Investigation of adsorption parameters for platinum and palladium onto a modified polyacrylonitrile-based sorbent. Int. J. Miner. Process. 137, 52–58.

Mao, J., Lin, S., Lu, X., Wu, X., Zhou, T., Yun, Y.-S., 2020. Ion-imprinted chitosan fiber for recovery of Pd(II): Obtaining high selectivity through selective adsorption and two-step desorption. Environ. Res. 182, 108995.

Oveisi, M., Asli, M.A., Mahmoodi, N.M., 2017. MIL-Ti metal-organic frameworks (MOFs) nanomaterials as superior adsorbents: synthesis and ultrasound-aided dye adsorption from multicomponent wastewater systems. J. Hazard. Mater. 347, 123–140.

Ozturk, N., Bulut, V.N., Duran, C., Soylak, M., 2011. Coprecipitation of palladium(II) with 1,5-diphenylcarbazite–copper(II) and determination by flame atomic absorption spectrometry. Desalination 270, 130–134.

Pang, H., Huang, S., Wu, Y., Yang, D., Wang, X., Yu, S., Chen, Z., Alsaedi, A., Hayat, T., Wang, X., 2018. Efficient elimination of U (VI) by polyethyleneimine-decorated fly ash. Inorg. Chem. Front. 5, 2399–2407.

Park, S.I., Kwak, I.S., Bae, M.A., Mao, J., Won, S.W., Han, D.H., Chung, Y.S., Yun, Y.S., 2012. Recovery of gold as a type of porous fiber by using biosorption followed by incineration. Bioresour. Technol. 104, 208–214.

Ramesh, A., Hasegawa, H., Sugimoto, W., Maki, T., Ueda, K., 2008. Adsorption of gold(III), platinum(IV) and palladium(II) onto glycine modified crosslinked chitosan resin. Bioresour. Technol. 99, 3801–3809.

Saleem, H., Rafique, U., Davies, R.P., 2016. Investigations on post-synthetically modified UiO-66-NH 2 for the adsorptive removal of heavy metal ions from aqueous solution. Microporous Mesoporous Mater. 221, 238–244.

Sarker, M., Ahmed, I., Jhung, S.H., 2017. Adsorptive removal of herbicides from water over nitrogen-doped carbon obtained from ionic liquid@ZIF-8. Chem. Eng. J. 323, 203–211.

Shahwan, T., 2014. Sorption kinetics: obtaining a pseudo-second order rate equation based on a mass balance approach. J. Environ. Chem. Eng. 2, 1001–1006.

Sharma, S., Rajesh, N., 2016. Augmenting the adsorption of palladium from spent catalyst using a thiazole ligand tethered on an amine functionalized polymeric resin. Chem. Eng. J. 283, 999–1008.

Srivastava, V., Shekhar, M., Gusain, D., Gode, F., Sharma, Y.C., 2017. Application of a heterogeneous adsorbent (HA) for the removal of hexavalent chromium from aqueous solutions: Kinetic and equilibrium modeling. Arabian J. Chem. 10, S3073–S3083.

Tang, F., Huang, X., Zhang, Y., Guo, J., 2000. Effect of dispersants on surface chemical properties of nano-zirconia suspensions. Ceram. Int. 26, 93–97.

Tanzifi, M., Hosseini, S.H., Kiadehi, A.D., MartinOlazar, K., Rezaiemehr, R., Ali, I., 2017. Artificial neural network optimization for methyl orange adsorption onto polyaniline nano-adsorbent: Kinetic, isotherm and thermodynamic studies. J. Mol. Liquids 244, 189–200.

Truong, H.T., Lee, M.S., 2018. Separation of Pd(II) and Pt(IV) from hydrochloric acid solutions by solvent extraction with Cyanex 301 and LIX 63. Miner. Eng. 115, 13–20.

Wang, C., Boithias, L., Ning, Z., Han, Y., Sauvage, S., Sánchez-Pérez, J.M., Kuramochi, K., Hatano, R., 2016. Comparison of Langmuir and Freundlich adsorption equations within the SWAT-K model for assessing potassium environmental losses at basin scale. Agric. Water Manag. 180, 205–211.

Wang, L., Sun, Y., Wang, J., Wang, J., Yu, A., Zhang, H., Song, D., 2010. Water-soluble ZnO–Au nanocomposite-based probe for enhanced protein detection in a SPR biosensor system. J. Colloid Interface Sci. 351, 392–397.

Wang, J., Li, Y., Lv, Z., Xie, Y., Shu, J., Alsaedi, A., Hayat, T., Chen, C., 2019. Exploration of the adsorption performance and mechanism of zeolitic imidazolate framework-8@graphene oxide for Pb (II) and 1-naphthylamine from aqueous solution. J. Colloid Interface Sci. 542, 410–420.

Wu, Y., Li, B., Wang, X., Yu, Pnag H., Liu, Y., Liu, X., Wang, X., 2019. Magnetic metal-organic frameworks (Fe3O4@ZIF-8) composites for U(VI)and Eu(III) elimination: simultaneously achieve favorable stability and functionality. Chem. Eng. J. 378 (2019).

Won, S.W., Kim, S., Kotte, P., Lim, A., Yun, Y.S., 2013. Cationic polymer-immobilized polysulfone-based fibers as high performance sorbents for Pt(IV) recovery from acidic solutions. J. Hazard. Mater. 263, 391–397.

Won, S.W., Park, J., Mao, J., Yun, Y.S., 2011. Utilization of PEI-modified Corynebacterium glutamicum biomass for the recovery of Pd(II) in hydrochloric solution. Bioresour. Technol. 102, 3888–3893.

Xavier, R.J., Gobinath, E., 2012. FT-IR, FT-Raman, ab initio and DFT studies, HOMO-LUMO and NBO analysis of 3-amino-5-

mercapto-1,2,4-triazole. Spectrochim. Acta Part A Mol. Biomol. Spectrosc. 86, 242–251.

Xie, F., Fan, R., Yi, Q., Fan, Z., Zhang, Q., Luo, Z., 2016. Adsorption recovery of Pd(II) from aqueous solutions by persimmon residual based bio-sorbent. Hydrometallurgy 165, 323–328.

Xie, Q., Lin, T., Chen, F., Wang, D., Yang, B., 2018. Recovery of ultra-trace palladium using chitosan and its sulphur-containing derivative in HCl medium. Hydrometallurgy 178, 188–194.

Xu, W.L., Fang, C., Zhou, F., Song, Z., Liu, Q., Qiao, R., Yu, M., 2017. Self-assembly: a facile way of forming ultrathin, high-performance graphene oxide membranes for water purification. Nano Lett. 17, 2928–2933.

Yao, B.J., Jiang, W.L., Dong, Y., Liu, Z.X., Dong, Y.B., 2016. Post-synthetic polymerization of UiO-66-NH2 nanoparticles and polyurethane oligomer toward stand-alone membranes for dye removal and separation. Chem. – Eur. J. 22, 10565–10571.

Yu, S., Wei, D., Shi, L., Ai, Y., Zhang, P., Wang, X., 2019. Three-dim ensional graphene/titanium dioxide composite for enhanced U(VI) capture: insights from batch experiments, XPS spectroscopy and DFT calculation. Environ. Pollut. 251, 975–983.

Yi, Q., Fan, R., Xie, F., Min, H., Zhang, Q., Luo, Z., 2016. Selective recovery of Au(III) and Pd(II) from waste PCBs using ethylene-diamine modified persimmon tannin adsorbent. Proc. Environ. Sci. 31, 185–194.

Zhu, K., Chen, C., Xu, H., Gao, Y., Tian, X., Alsaedi, A., Hayat, T., 2017. Cr(VI) reduction and immobilization by core-double-shell structured magnetic polydopamine@zeolitic idazolate frameworks-8 microspheres. ACS Sustain. Chem. Eng. 5, 6795–6802.

Zhang, Z., Zhang, X., Niu, D., Li, Y., Shi, J., 2017. Highly efficient and selective removal of trace lead from aqueous solutions by hollow mesoporous silica loaded with molecularly imprinted polymers. J. Hazard. Mater. 328, 160–169.

Zhou, L., Zhang, X., Chen, Y., 2017. Facile synthesis of Al-fumarate metal–organic framework nano-flakes and their highly selective adsorption of volatile organic compounds. Mater. Lett. 197, 224–227.